

Cusp-core problem and strong gravitational lensing *

Nan Li and Da-Ming Chen

National Astronomical Observatories, Chinese Academy of Sciences, Beijing 100012, China;
uranus@bao.ac.cn; cdm@bao.ac.cn

Received 2009 May 12; accepted 2009 May 18

Abstract Cosmological numerical simulations of galaxy formation have led to the cuspy density profile of a pure cold dark matter halo toward the center, which is in sharp contradiction with the observations of the rotation curves of cold dark matter-dominated dwarf and low surface brightness disk galaxies, with the latter tending to favor mass profiles with a flat central core. Many efforts have been devoted to resolving this cusp-core problem in recent years, among them, baryon-cold dark matter interactions are considered to be the main physical mechanisms erasing the cold dark matter (CDM) cusp into a flat core in the centers of all CDM halos. Clearly, baryon-cold dark matter interactions are not customized only for CDM-dominated disk galaxies, but for all types, including giant ellipticals. We first fit the most recent high resolution observations of rotation curves with the Burkert profile, then use the constrained core size-halo mass relation to calculate the lensing frequency, and compare the predicted results with strong lensing observations. Unfortunately, it turns out that the core size constrained from rotation curves of disk galaxies cannot be extrapolated to giant ellipticals. We conclude that, in the standard cosmological paradigm, baryon-cold dark matter interactions are not universal mechanisms for galaxy formation, and therefore, they cannot be true solutions to the cusp-core problem.

Key words: cosmology: dark matter — galaxies: formation — galaxies: halos — galaxies: structure — gravitational lensing

1 INTRODUCTION

In the standard Λ cold dark matter cosmology paradigm (called Λ CDM), the observed large scale structure (LSS) of the universe, which is composed of virialized galaxies and clusters of galaxies, is hierarchically formed from primordial density fluctuations in the early universe (e.g., Longair 2008). During the matter dominated epoch, CDM overdensities provide deep enough gravitational potentials so that small dark halos can form, merge and evolve more rapidly (compared with only baryons) to make the present LSS. It is believed that, during the whole structure formation process, baryons follow CDM potentials and then reside at the centers of their host dark halos. As a result, each galaxy or cluster of galaxies is surrounded by a dark matter halo. In the framework of Λ CDM N-body numerical simulations, some analytical and semi-analytical models have successfully predicted most of the observational properties of LSS. However, challenges arise from small, galactic scales. Numerical simulations predict too many substructures (dwarf galaxies), e.g., several hundreds of satellites are predicted in a galaxy like our Milky Way, while only 23 of them are observed; too low angular momenta of spiral galaxies; and too high densities (cusps) in the galactic centers (Navarro et al. 1997; Jing 2000; Navarro et al. 2004; Jing &

* Supported by the National Natural Science Foundation of China.

Suto 2002), whereas high resolution observations of the rotation curves for CDM-dominated dwarf and low surface brightness (LSB) galaxies imply that galactic dark matter halos have a density profile with a flat central core (de Blok et al. 2001b; van den Bosch & Swaters 2001; Swaters et al. 2003; Woldrake et al. 2003; Donato et al. 2004; Gentile et al. 2005; Simon et al. 2005; Gentile et al. 2007). The latter is known as the cusp-core problem, which we will investigate in detail in this paper.

Many efforts have been devoted to resolving the challenges mentioned above. The less traditional models include warm dark matter and self-interacting dark matter. In the LCDM model, some researchers simply deny the validity of the observations, others introduce baryon-cold dark matter interactions (BCDMIs) such as dynamical friction of substructures (El-Zant et al. 2001; Tonini et al. 2006; Romano-Diaz et al. 2008), stellar bar-CDM interaction (Weinberg & Katz 2002; Holley-Bockelmann et al. 2005), and baryon energy feedback (Mashchenko et al. 2006; Peirani et al. 2008). In this paper, we focus on the validity of BCDMI solutions to the cusp-core problem.

First of all, we point out that any reasonable solutions to the cusp-core problem should be verified by the observations of galaxies not only on small scales like dwarf and LSBs, but rather on all galactic scales, especially on scales like giant ellipticals. Why should we include the giant ellipticals when testing structure formation models (e.g., the solutions to the cusp-core problem)? According to the hierarchical structure formation theory in the frame work of LCDM, small CDM halos form first, then merge to make increasingly larger halos. While N-body numerical simulations of pure CDM with higher and higher force and mass resolution still favor cuspy halo profiles, the BCDMIs introduced in the baryon plus CDM regime can transfer the early formed cusp into a central flat core in later stages for each dark halo. It is well known that the “universal” density profile known as NFW (Navarro-Frenk-White; Navarro et al. 1997) is valid for halos ranging from dwarf galaxies to those as large as clusters of galaxies. The only difference between pure CDM and baryon plus CDM regimes is that the latter considers the effects of baryons. Their formation processes should be similar (bottom-up or hierarchical) in the spirit of LCDM. Therefore, the properties of the galaxies (e.g., the slope in the central region) predicted by BCDMIs should be valid and meaningful at all mass scales. Needless to say, for any theoretical models describing structure formation, it is meaningless or impossible to customize some physical processes only to explain the observations of dwarfs and LSBs, and exclude ellipticals as exceptions. In other words, no matter what galaxy types the initial conditions presumed, the subsequential and final (present) CDM halos predicted by simulations should include all galaxy types and have the same observational properties. This is why we should include giant ellipticals when testing solutions to the cusp-core problem. Usually, when we talk about the cusp-core problem, we mean the contradiction between the “cusp” predicted by simulations of pure CDM and the “core” implied by rotation curves of dwarfs and LSBs, as is widely known. However, we forget the fact that giant elliptical galaxies are also important members of the galactic family, but they prefer a cuspy (or small core-size) density profile in their central region according to observations (e.g., X-rays and the statistics of strong gravitational lensing). Indeed, LSB galaxies and giant ellipticals are quite different galaxies; the former are CDM-dominated while the latter have baryon-dominated centers. However, their distinguishing differences are obtained from all kinds of observational data rather than theoretically predicted from structure formation theories. It is theories that should successfully explain such observational differences, not the other way around. The density profiles of giant ellipticals with baryon-dominated centers (a cusp or small core) should be predicted by the same model, if reasonable, which predicts the density profile of LSB galaxies with CDM-dominated centers (a large flat core).

It is interesting to note that some solutions to the cusp-core problem based on analytical models are problematic in a similar way to simulations. One such model assumes that cosmological halos form from the collapse and virialization of “top-hat” density perturbations and are spherical, isotropic and isothermal. This predicts a unique, nonsingular, truncated isothermal sphere (NTIS) and provides a simple physical clue about the existence of soft cores in halos of cosmological origin (Shapiro et al. 1999; Iliev & Shapiro 2001). It is claimed that this NTIS model is in good agreement with observations of the internal structure of dark matter-dominated halos on scales ranging from dwarf galaxies to X-ray clusters. Unfortunately, the NTIS model is ruled out by the statistics of strong gravitational lensing (Chen 2005).

In summary, any self-consistent, reasonable solutions to the cusp-core problem, either numerical or analytical, should be able to successfully explain the cuspy density profiles of giant ellipticals simultaneously, otherwise, no matter how reasonable it looks, such a solution cannot be true.

While giant ellipticals should be included, now the question is: to what extent is the core size of the giant ellipticals allowed by observations? In particular, is it acceptable to extrapolate the core size-halo mass relation constrained by the rotation curves of dwarfs and LSB galaxies to giant ellipticals? Like Chen & McGaugh (2008), we investigate these problems by “reasonably” extrapolating the core-mass relation constrained from LSB galaxies to strong lensing galaxies (usually ellipticals), and comparing the predicted lensing frequency with observations. Since it was explicitly pointed out in Mashchenko et al. (2006) that the CDM density profile of the evolved halo is in remarkable agreement with the Burkert profile, we fit the observational data of rotation curves with the Burkert density profile in Section 2, the corresponding lensing probabilities are presented in Section 3, and we give our discussion and conclusions in Section 4.

2 DENSITY PROFILE CONSTRAINED FROM OBSERVATIONS OF ROTATION CURVES

We use high-resolution and high-quality hybrid $H_\alpha/H\text{ I}$ rotation curves of a sample of 26 LSB galaxies, analyzed in de Blok et al. (2001a), to fit the parameters in the Burkert density profile (Burkert 1995). Some curves of this sample were taken from the large sample of 50 LSB galaxies presented in McGaugh et al. (2001). While these curves were well fitted by the cored isothermal sphere model (Begeman et al. 1991; de Blok & Bosma 2002; Kuzio de Naray et al. 2008), we will show below that they are also well fitted by the Burkert density profile (see also Salucci & Burkert 2000; Gentile et al. 2004; Salucci et al. 2007). As a typical model of BCDMIs, turbulence driven by stellar feedback during galaxy formation is a possible solution to the cusp-core problem (Mashchenko et al. 2006). Numerical N-body simulations show us that random bulk motions of gas in small primordial galaxies result in a flattening of the central CDM cusp. Phase space arguments imply that the core should persist through subsequent mergers (Dehnen 2005; Kazantzidis et al. 2006). Consequently, in the present universe, both small and large galaxies would have flat CDM core density profiles, which can be well fitted with the Burkert model (Burkert 1995; Mashchenko et al. 2006),

$$\rho(r) = \frac{\rho_0 r_0^3}{(r + r_0)(r^2 + r_0^2)}, \quad (1)$$

where ρ_0 is the central density near $r = 0$ and r_0 is the core radius, with two free parameters to be fitted. The mass within radius r is (Salucci et al. 2007),

$$M(r) = 2\pi\rho_0 r_0^3 \left\{ \ln\left(1 + \frac{r}{r_0}\right) + \ln\left[1 + \left(\frac{r}{r_0}\right)^2\right] - \arctan\left(\frac{r}{r_0}\right) \right\}. \quad (2)$$

The corresponding orbital velocity at radius r is simply $V^2(r) = GM(r)/r$, where G is the gravitational constant. The sample (de Blok et al. 2001a) provides for each galaxy the observed velocity V (km s^{-1}) and uncertainty V_{Err} (km s^{-1}) at radius r (kpc^{-1}). We fit the rotation curves with $V^2(r, \rho_0, r_0)$ and derive the values of the parameter pair (ρ_0, r_0) for each galaxy of the sample. Figure 1 shows the fitted $V^2(r)$ (solid lines) and the observed data of rotation curves (crosses) for each galaxy. Note that, for a few galaxies, especially F579, U11648 and U11748, the Burkert-fitted lines (solid) deviate greatly from the data points at large radii. However, this will not affect our further analysis, because our interests are focused on the central regions, where the data have been well-fitted. Statistically, there is a correlation between ρ_0 and r_0 for the sample; the fitted result is

$$\rho_0 = 0.029 \left(\frac{r_0}{\text{kpc}}\right)^{-1/2} M_\odot \text{pc}^{-3}. \quad (3)$$

In later lens probability calculations, we need to know the total virialized halo mass $M = M_{\text{vir}}$. For the Burkert profile, the mass diverges logarithmically at large radii, and should be cut off at r_{200} , the

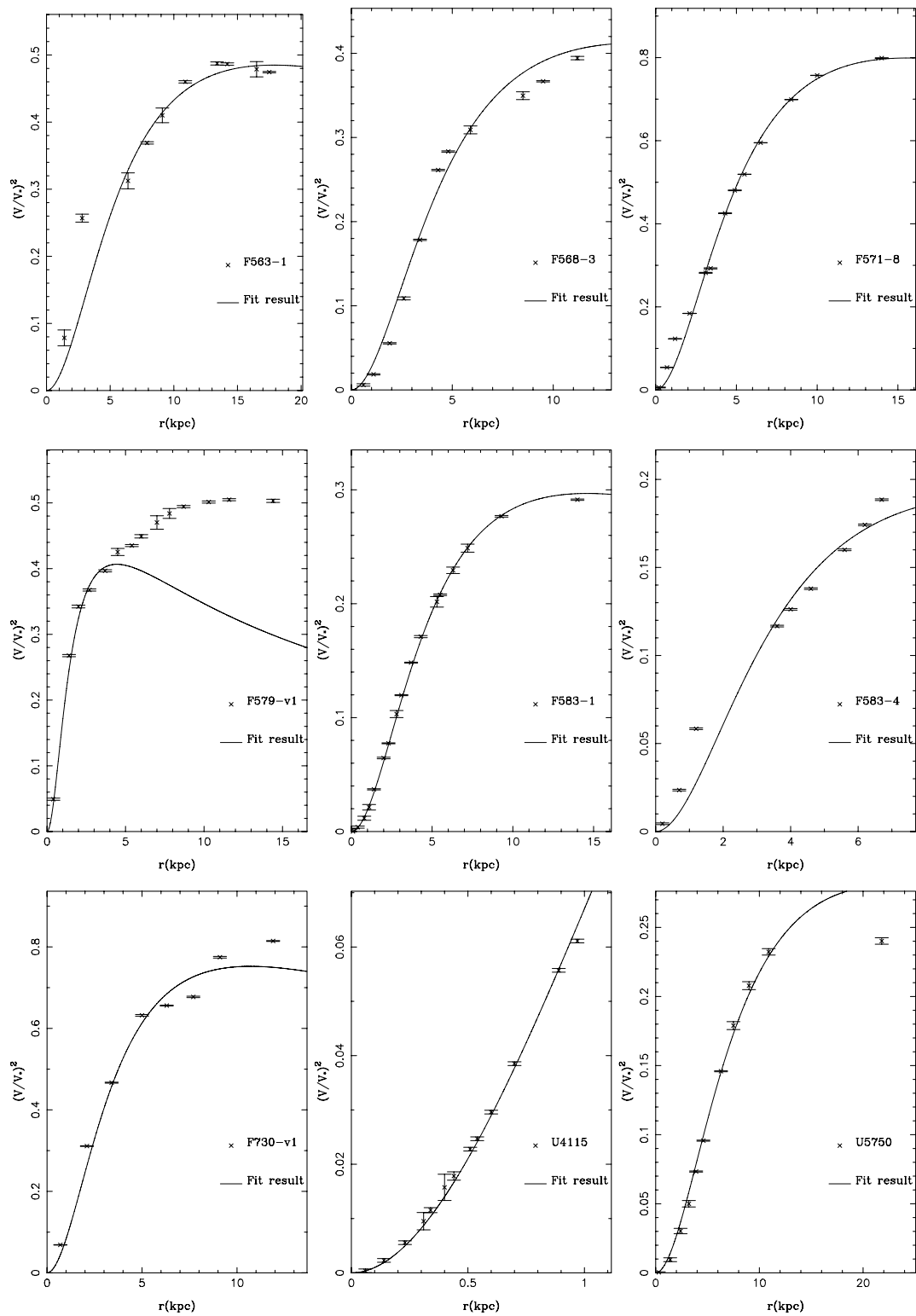


Fig. 1 Comparison of the fitted $(V(r)/V_*)^2$, $V_* = 161 \text{ km s}^{-1}$, derived from the Burkert profile (*solid lines*) and the observed rotation curves (*crosses*).

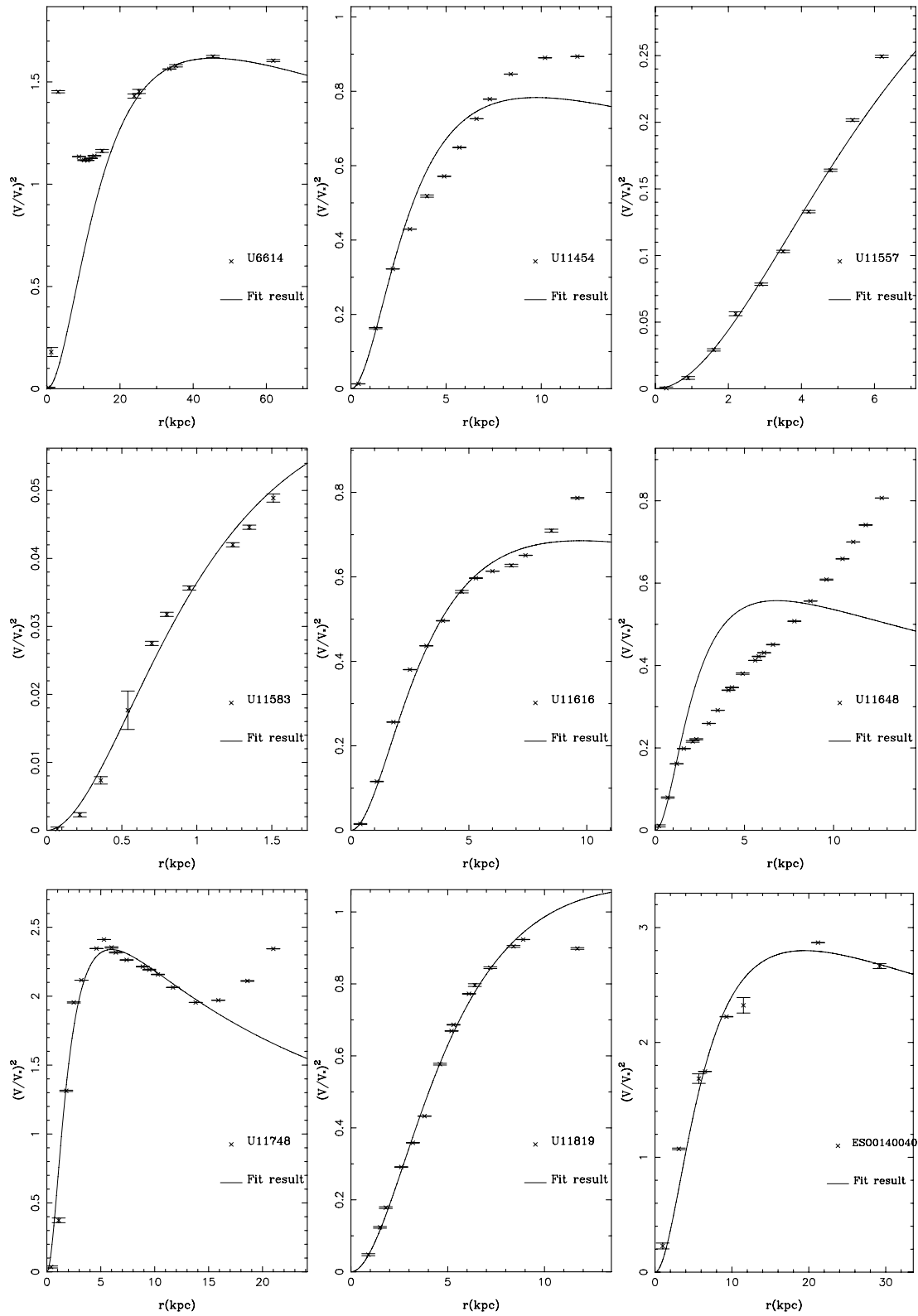


Fig. 1 — Continued.

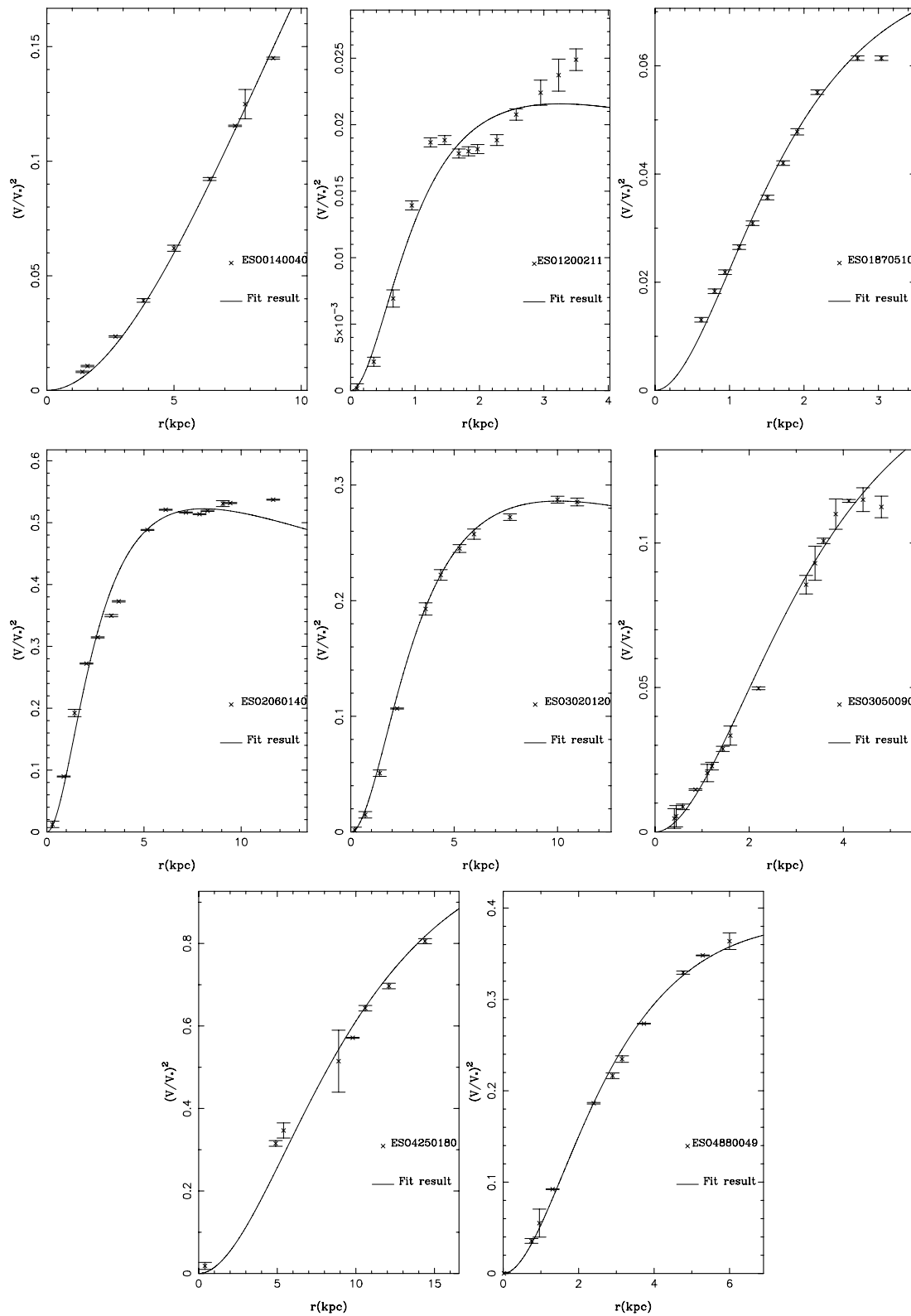


Fig. 1 — Continued.

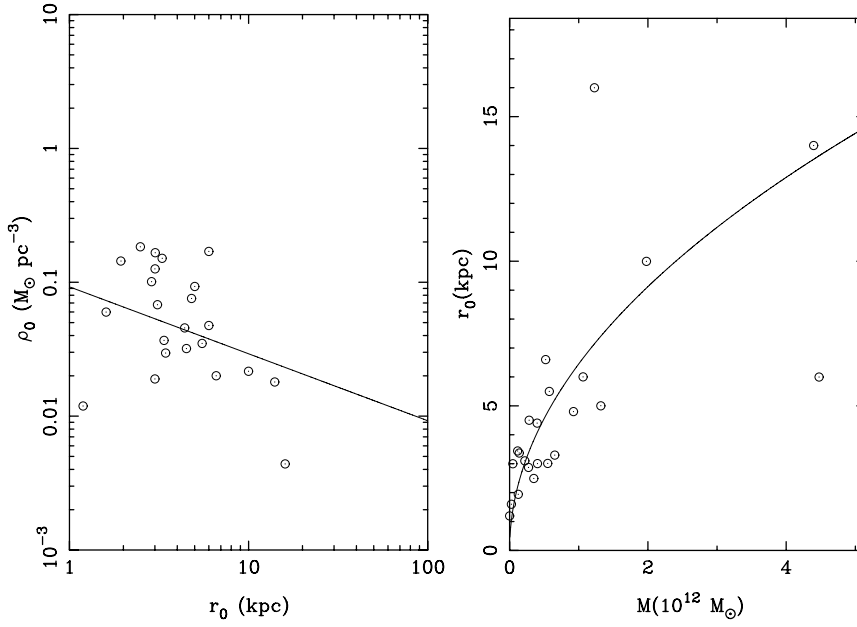


Fig. 2 *Left panel:* the correlation between central density ρ_0 and core radius r_0 ; crosses represent the data derived from the rotation curves of the sample with the Burkert profile, the solid line is the fit with the data. *Right panel:* the relation between core radius r_0 and the virialized halo mass M .

radius of a sphere within which the average mass density is 200 times the critical density of the universe, typically taken as the virial radius (Navarro et al. 1997). So, we define

$$M \equiv M_{\text{vir}} = M_{200} = M(r_{200}) = \frac{800\pi\rho_{\text{crit}}(z)}{3}r_{200}^3, \quad (4)$$

where $M(r_{200})$ is the virialized halo mass obtained by substituting $r = r_{200}$ into Equation (2), and $\rho_{\text{crit}}(z)$ is the critical density of the universe at redshift z . By numerically solving Equations (3) and (4), we get an approximate relation between r_0 and M ,

$$r_0 = 6.45 \left(\frac{M}{10^{12}M_\odot} \right)^{1/2} \text{ kpc}, \quad (5)$$

which is similar to the result of Salucci et al. (2007), although we have adopted different procedures and used different samples. The correlations between the pairs (ρ_0, r_0) and (r_0, M) are presented in Figure 2.

3 STRONG LENSING PROBABILITIES

It has been explicitly pointed out (Mashchenko et al. 2006) that, on one hand, the resultant cored dark matter halos produced by stellar feedback are in agreement with the Burkert profile, and on the other hand, as the dwarf galaxies merge together to make larger ones, the flat-cored shape of the dark matter density profile is preserved in subsequent massive halos. Therefore, in this section, we assume that the Burkert profile constrained from the rotation curves of the LSB galaxies in the previous section is also appropriate for strong lensing galaxies (usually giant ellipticals), and we use it to calculate the corresponding lensing frequency.

Gravitational lensing provides a powerful and independent tool to detect the matter distribution in LSS (Schneider et al. 1992; Wambsganss et al. 1995; Wu 1996, 2000, 2004; Bartelmann 1996; Bartelmann & Schneider 2001; Keeton 2001, 2002, 2003; Keeton & Zabludoff 2004; Zhang et al. 2003, 2009). In particular, by virtue of eliminating the degeneracy of some lens and cosmological models, strong lensing statistics exhibits an exceptional ability to investigate both dark matter (Turner et al. 1984; Wu 1993; Chae et al. 2002; Li & Ostriker 2002, 2003; Chae 2003; Chen 2003a,b, 2005; Chen & Zhao 2006; Chen 2008; Oguri et al. 2002; Oguri 2003; Oguri et al. 2003; Zhang 2004; Chae 2007) and dark energy (Fukugita et al. 1990; Fukugita, & Turner 1991; Turner 1990; Krauss & White 1992; Maoz & Rix 1993; Wu 1993; Kochanek 1995, 1996; Falco et al. 1998; Cooray & Huterer 1999; Waga & Miceli 1999; Sarbu, Rusin, & Ma 2001; Chen 2004a,b; Dev et al. 2004; Yang & Chen 2009; Zhang, Cheng & Wu 2009). With the increasing number of the newly discovered lenses (e.g., Wen et al. 2009), we now have at least two well-defined statistical lens samples. In addition to the radio lens sample (CLASS/JVAS ; Patnaik et al. 1992; King et al. 1999; Myers et al. 2003; Browne et al. 2003), we have a Sloan Digital Sky Survey Quasar Lens Search Data Release 3 (SQLS DR3; Inada et al. 2008) optical lens sample, which first included a cluster-scale lens, and thus provides stronger constraints on halo models, especially for the universal properties of halos ranging from dwarf galaxies to clusters of galaxies (Oguri et al. 2008; Oguri & Blandford 2009).

The lens equation is $\eta = D_S \xi / D_L - D_{LS} \hat{\alpha}$, where η and ξ are the physical positions of a source in the source plane and an image in the image plane, respectively, $\hat{\alpha}$ is the deflection angle, and D_L , D_S , and D_{LS} are the angular diameter distances from observer to lens, observer to source, and lens to source, respectively. By defining dimensionless positions $y = D_L \eta / D_S r_0$ and $x = \xi / r_0$, and dimensionless angle $\alpha = D_L D_{LS} \hat{\alpha} / D_S r_0$, the lens equation is then $y = x - \alpha$. For a circularly symmetric lens, $\hat{\alpha} = 4GM(\xi)/c^2\xi$, where $M(\xi)$ is the mass within a circle of radius ξ (Schneider et al. 1992). For the Burkert profile, $M(x) = 4\pi\rho_0 r_0^3 m(x)$ (Park & Ferguson 2003), where

$$m(x) = \begin{cases} \ln \frac{x}{2} + \frac{\pi}{4}(\sqrt{x^2+1}-1) + \frac{\sqrt{x^2+1}}{2} \operatorname{arccoth}(\sqrt{x^2+1}) \\ - \frac{1}{2}\sqrt{x^2-1} \arctan \sqrt{x^2-1}, & \text{if } x > 1, \\ -\ln 2 - \frac{\pi}{4} + \frac{1}{2\sqrt{2}}[\pi + \ln(3+2\sqrt{2})], & \text{if } x = 1, \\ \ln \frac{x}{2} + \frac{\pi}{4}(\sqrt{x^2+1}-1) + \frac{\sqrt{x^2+1}}{2} \operatorname{arccoth}(\sqrt{x^2+1}) \\ + \frac{1}{2}\sqrt{1-x^2} \operatorname{arctanh}\sqrt{1-x^2}, & \text{if } x < 1. \end{cases}$$

The lens equation for the Burkert profile then is

$$y = x - \frac{8\kappa_c m(x)}{\pi x}, \quad \kappa_c = \left(\frac{2\pi^2 G \rho_0 r_0}{c^2} \right) \left(\frac{D_L D_{LS}}{D_S} \right) = \frac{\Sigma(0)}{\Sigma_{\text{crit}}}, \quad (6)$$

where κ_c is the central convergence, an important quantity that determines whether strong lensing can occur or not, $\Sigma(0) = \pi\rho_0 r_0/2$ is the surface mass density at the lens center and $\Sigma_{\text{crit}} = c^2 D_S / 4\pi G D_L D_{LS}$ is the critical surface density.

Generally, for any spherically symmetric density profiles of lensing halos, multiple images can be produced only if the central convergence κ_c is greater than unity (Schneider et al. 1992). When $\kappa_c \leq 1$, only one image is produced. Note that even if $\kappa_c > 1$ is satisfied, multiple images can occur only when the source is located within $y_{\text{cr}} = y(x_{\text{cr}})$ (Li & Ostriker 2002), where x_{cr} is determined from Equation (6), with $dy/dx = 0$ for $x < 0$ (this is similar to lensing by cored isothermal sphere halos, see Chen 2005). For a singular density profile such as the singular isothermal sphere (SIS) and NFW profiles, the central value is divergent, so $\kappa > 1$ is always satisfied, and multiple images can be produced for any given mass. For density profiles with a finite soft core, such as core isothermal spheres, NTIS and Burkert profiles, however, the condition $\kappa > 1$ requires that only halos with mass greater than a certain value (determined by $\kappa_c = 1$) can produce multiple images.

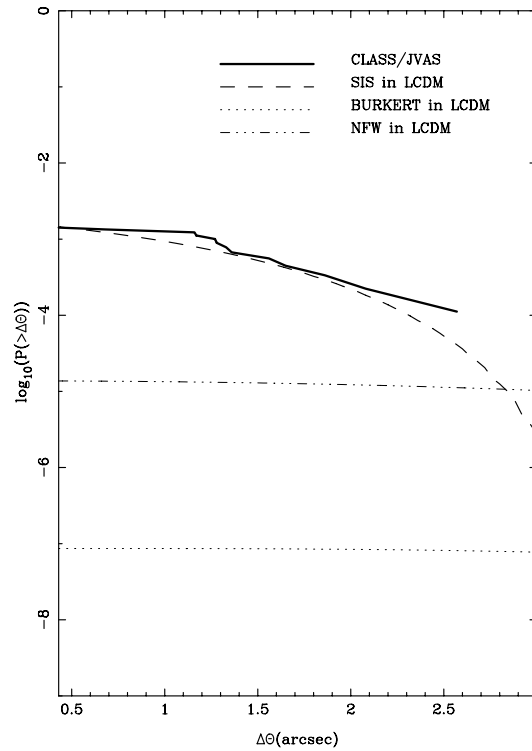


Fig. 3 Lensing probability with image separation larger than $\Delta\theta$. Our predicted lensing probability based on the Burkert model (*dotted line*) is about four orders of magnitude lower than the observations of CLASS/JVAS (*thick histogram*). As expected, the SIS model (*dashed line*) is in very good agreement with observations. The NFW model (*dash-dotted*) also fails to explain observations but is much better than the Burkert model.

The calculations for lensing probabilities with quasars at redshift z_s lensed by Burkert halos of galaxies and with image separations larger than $\Delta\theta$ are straightforward (see Chen 2005, for details),

$$P(> \Delta\theta) = 0.06 y_{\text{cr}} \int_0^{1.27} (1+z)^3 \frac{dD_L^P(z)}{dz} dz \int_{M_{\text{min}}(\Delta\theta, z)}^{\infty} f(M, z) dM \int_0^{y_{\text{cr}}} y [\mu(y)]^{1.1} dy, \quad (7)$$

where $D_L^P(z)$ is the proper distance from the observer to the lens located at redshift z ; $f(M, z)$ is the mass function, for which we use the expression given by Jenkins et al. (2001); $M_{\text{min}}(\Delta\theta, z)$ is the minimum mass of halos above which lenses can produce images with separations greater than $\Delta\theta$; and $\mu(y)$ is the total magnification of the two outer images for a source at y , which can be calculated directly from the lens equation (6).

In our actual numerical calculations, we choose almost the same procedures, mass function and even background universe as in Chen (2005), except for the distribution of the redshifts of source quasars, for which, as in Chen & McGaugh (2008), we use only the mean value $z_s = 1.27$. The result is shown in Figure 3. The observational result for the well defined combined sample of the cosmic Lens All-Sky Survey (CLASS) and Jodrell Bank/Very Large Array Astrometric Survey (JVAS) is shown as a thick histogram (see Chen 2005, and references therein). For comparison, the lensing probability of the SIS model and NFW model are also shown with the same parameters and approximations as Burkert.

4 DISCUSSION AND CONCLUSIONS

We have calculated the lensing probability based on the Burkert profile model, for which the core size-halo mass relation is obtained by fitting the high-resolution rotation curves of a sample containing 26 galaxies. For comparison, we have recalculated the lensing probability for the SIS model and NFW model with the same parameters and approximations as Burkert. As expected, the lensing probability for the Burkert model is 4 orders of magnitude lower than the observations of CLAS/JVAS. While our strong lensing calculations rule out the Burkert model as a possible giant elliptical density profile, we conclude, at the same time, that the stellar feedback mechanisms (Mashchenko et al. 2006; Peirani et al. 2008) are also ruled out as reasonable solutions to the cusp-core problem. Additionally, this conclusion is independent of the models used to fit rotation curves: Burkert in this paper, and cored isothermal spheres (Kuzio de Naray et al. 2008) in Chen & McGaugh (2008).

Other solutions to the cusp-core problem, including the analytical NTIS model (Shapiro et al. 1999; Iliev & Shapiro 2001; Chen 2005), dynamical friction of substructures (El-Zant et al. 2001; Tonini et al. 2006; Romano-Diaz et al. 2008) and stellar bar-CDM interaction (Weinberg & Katz 2002; Holley-Bockelmann et al. 2005), face exactly the same embarrassing problem. Clearly, the solutions proposed so far can produce a large core for each dwarf and LSB galaxy, and thus can successfully explain the observations of rotation curves, but they cannot explain the steep and cuspy centers of massive galaxies, which are favored by strong lensing and X-ray observations. As a matter of fact, in the framework of LCDM, the so called “cusp-core problem” encountered by hierarchical structure formation theories is not just the contradiction between the cusp predicted by pure CDM simulations and the core implied by the observations of rotation curves, but rather, the cusp predicted by pure CDM simulations on all mass scales, the core implied by rotation curves on small, dwarf galaxy scales and the cusp favored by strong lensing and X-ray observations on large, giant elliptical galaxy scales. From an observational point of view, regardless of theories, we can call this the “cusp-core phenomena” rather than “problem,” when referring to the cusp in large scale galaxies and the core in small scale galaxies. As we have pointed out, a reasonable, self-consistent theory should explain the observations on all mass scales, i.e., all “cusp-core phenomena,” rather than only the cores on small scales.

Acknowledgements We are indebted to Stacy McGaugh for providing us with detailed data of the rotation curves of the sample, and we are grateful to the anonymous referee for helpful suggestions and comments. This work was supported by the National Natural Science Foundation (Grant No. 10673012), CAS (Grant No. KJCX3-SYW-N2) and the National Basic Research Program of China (973 Program; Grant No. 2009CB24901).

References

- Bartelmann, M. 1996, *A&A*, 313, 697
 Bartelmann, M., & Schneider, P. 2001, *Phys. Rept.*, 340, 291
 Begeman, K. G., Broeils, A. H., & Sanders, R. H. 1991, *MNRAS*, 249, 523
 Browne, I. W. A., et al. 2003, *MNRAS*, 341, 13
 Burkert, A. 1995, *ApJ*, 447, L25
 Chae, K. -H., et al. 2002, *Phys. Rev. Lett.*, 89, 151301
 Chae, K. -H. 2003, *MNRAS*, 346, 746
 Chae, K. -H. 2007, *ApJ*, 658, L71
 Chen, D. -M. 2003a, *A&A*, 397, 415
 Chen, D. -M. 2003b, *ApJ*, 587, L55
 Chen, D. -M. 2004a, *A&A*, 418, 387
 Chen, D. -M. 2004b, *ChJAA (Chin. J. Astron. Astrophys.)*, 4, 118
 Chen, D. -M. 2005, *ApJ*, 629, 23
 Chen, D. -M. 2008, *JCAP*01, 006
 Chen, D. -M., & McGaugh, S. 2008, *ArXiv e-prints (arXiv: 0808.0225)*
 Chen, D. -M., & Zhao, H. 2006, *ApJ*, 650, L9

- Cooray, A. R., & Huterer, D. 1999, *ApJ*, 513, L95
- de Blok, W. J. G., & Bosma, A. 2002, *A&A*, 385, 816
- de Blok, W. J. G., McGaugh, S., & Rubin, V. C. 2001, *AJ*, 122, 2396
- de Blok, W. J. G., McGaugh, S., Bosma, A., & Rubin, V. C. 2001, *ApJ*, 552, L23
- Dehnen, W. 2005, *MNRAS*, 360, 892
- Dev, A., Jain, D., & Alcaniz, J. S. 2004, *A&A*, 417, 847
- Donato, F., Gentile, G., & Salucci, P. 2004, *MNRAS*, 353, 17
- El-Zant, A., Shlosman, I., & Hoffman, Y. 2001, *ApJ*, 560, 636
- Falco, E. E., Kochanek, C. S., & Muñoz, J. A. 1998, *ApJ*, 494, 47
- Fukugita, M., Futamase, T., & Kasai, M. 1990, *MNRAS*, 246, 24P
- Fukugita, M., Turner, E. L. 1991, *MNRAS*, 253, 99
- Gentile, G., Salucci, P., Klein, U., Vergani, D., & Kalberla, P. 2004, *MNRAS*, 351, 903
- Gentile, G., Burkert, A., Salucci, P., Klein, U., & Walter, F. 2005, *ApJ*, 634, L145
- Gentile, G., Salucci, P., Klein, U., & Granato, G. L. 2007, *MNRAS*, 375, 199
- Holley-Bockelmann, K., Weinberg, M., & Katz, N. 2005, *MNRAS*, 363, 991
- Iliev, I. T., & Shapiro, P. R. 2001, *MNRAS*, 325, 468
- Inada, N., et al. 2008, *AJ*, 135, 496
- Jenkins, A., Frenk, C. S., White, S. D. M., Colberg, J. M., Cole, S., Evrard, A. E., Couchman, H. M. P., & Yoshida, N. 2001, *MNRAS*, 321, 372
- Jing, Y. 2000, *ApJ*, 535, 30
- Jing, Y. & Suto, Y. 2002, *ApJ*, 574, 538
- Kazantzidis, S., Zentner, A. R., & Kravtsov, A. V. 2006, *ApJ*, 641, 647
- Keeton, C. S. 2001, *ApJ*, 561, 46
- Keeton, C. R. 2002, *ApJ*, 575, L1
- Keeton, C. R. 2003, *ApJ*, 582, 17
- Keeton, C. R., & Zabludoff, A. I. 2004, *ApJ*, 612, 660
- King, L. J., Browne, I. W. A., Marlow, D. R., Patnaik, A. R., & Wilkinson, P. N. 1999, *MNRAS*, 307, 255
- Kochanek, C. S. 1995, *ApJ*, 453, 545
- Kochanek, C. S. 1996, *ApJ*, 466, 638
- Krauss, L. M., & White, M. 1992, *ApJ*, 394, 385
- Kuzio de Naray, R., McGaugh, S., & de Blok, W. J. G. 2008, *ApJ*, 676, 920
- Li, L. -X., & Ostriker, J. P. 2002, *ApJ*, 566, 652
- Li, L. -X., & Ostriker, J. P. 2003, *ApJ*, 595, 603
- Longair, M. S. 2008, *Galaxy Formation* (2nd ed.; Berlin: Springer-Verlag)
- Mashchenko, S., Wadsley, J., & Couchman, H. M. P. 2008, *Science*, 319, 174
- Maoz, D., & Rix, H. -W. 1993, *ApJ*, 416, 425
- McGaugh, S., Rubin, V. C., & de Blok, W. J. G. 2001, *AJ*, 122, 2381
- Myers, S. T., et al. 2003, *MNRAS*, 341, 1
- Navarro, J. F., Frenk, C. S., & White, S. D. M. 1997, *ApJ*, 490, 493
- Navarro, J. F., et al. 2004, *MNRAS*, 349, 1039
- Oguri, M. 2003, *MNRAS*, 339, L23
- Oguri, M., Suto, Y., & Turner, E. L. 2003, *ApJ*, 583, 584
- Oguri, M., Taruya, A., Suto, Y., & Turner, E. L. 2002, *ApJ*, 568, 488
- Oguri, M., et al. 2008, *AJ*, 135, 512
- Oguri, M., & Blandford, R. D. 2009, *MNRAS*, 392, 930
- Park, Y., & Ferguson, H. C. 2003, *ApJ*, 589, L65
- Patnaik, A. R., Browne, I. W. A., Wilkinson, P. N., & Wrobel, J. M. 1992, *MNRAS*, 254, 655
- Peirani, S., Kay, S., & Silk, J. 2008, *A&A*, 479, 123
- Romano-Diaz, E., Shlosman, I., Hoffman, Y., & Heller, C. 2008, *ApJ*, 685, L105
- Salucci, P., & Burkert, A. 2000, *ApJ*, 537, L9
- Salucci, P., Lapi, A., Tonini, C., Gentile, G., Yegorova, I., & Klein, U. 2007, *MNRAS*, 378, 41
- Sarbu, N., Rusin, D., & Ma, C.-P. 2001, *ApJ*, 561, L147

- Schneider, P., Ehlers, J., & Falco, E. E. 1992, *Gravitational Lenses* (Berlin: Springer-Verlag)
- Shapiro, P. R., Iliiev, I. T., & Raga, A. C. 1999, *MNRAS*, 307, 203
- Simon, J. D., Bolatto, A. D., Leroy, A., Blitz, L., & Gates, E. L. 2005, *ApJ*, 621, 757
- Swaters, R. A., Madore, B. F., van den Bosch, F. C., & Balcells, M. 2003, *ApJ*, 583, 732
- Tonini, C., Lapi, A., & Salucci, P. 2006, *ApJ*, 649, 591
- Turner, E. L. 1990, *ApJ*, 365, L43
- Turner, E. L., Ostriker, J. P., & Gott, J. R. 1984, *ApJ*, 284, 1
- van den Bosch, F. C., & Swaters, R. A. 2001, *MNRAS*, 325, 1017
- Waga, I., & Miceli, A. P. M. R. 1999, *Phys. Rev. D*, 59, 103507
- Wambsganss, J., Cen, R., Ostriker, J. P., & Turner, E. L. 1995, *Science*, 268, 274
- Weinberg, M. D., & Katz, N. 2002, *ApJ*, 580, 627
- Weldrake, D. T. F., de Blok, W. J. G., & Walter F. 2003, *MNRAS*, 340, 12
- Wen, Z. -L., Han, J.-L., Xu, X.-Y., et al. 2009, *RAA (Research Astron. Astrophys.)*, 9, 5
- Wu, X.-P., Hammer, F. 1993, *MNRAS*, 262, 187
- Wu, X.-P. 1996, *Fundam. Cosmic Phys.*, 17, 1
- Wu, X.-P. 2000, *MNRAS*, 316, 299
- Wu, X.-P. 2004, *MNRAS*, 349, 816
- Yang, X. J., & Chen, D. -M. 2009, *MNRAS*, 394, 1449
- Zhang, Q. J., Cheng, L. M., & Wu, Y. L., 2009, *ApJ*, 694, 1402
- Zhang, T. -J., Pen, U. -L., Zhang, P., & Dubinski, J. 2003, *ApJ*, 598, 818
- Zhang, T. -J. 2004, *ApJ*, 602, L5
- Zhang, T. J., Yuan, Q., & Lan, T. 2009, *New Astron.*, 14, 507